FULL PAPER

Far-Red Fluorescent Lipid-Polymer Probes for an Efficient Labeling of Enveloped Viruses

William Lacour, Salim Adjili, Julie Blaising, Arnaud Favier, Karine Monier, Sarra Mezhoud, Catherine Ladavière, Christophe Place, Eve-Isabelle Pécheur,* and Marie-Thérèse Charreyre*

Far-red emitting fluorescent lipid probes are desirable to label enveloped viruses, for their efficient tracking by optical microscopy inside autofluorescent cells. Most used probes are rapidly released from membranes, leading to fluorescence signal decay and loss of contrast. Here, water-soluble lipid-polymer probes are synthesized harboring hydrophilic or hydrophobic far-red emitting dyes, and exhibiting enhanced brightness. They efficiently label Hepatitis C Virus pseudo-typed particles (HCVpp), more stably and reproducibly than commercial probes, and a strong fluorescence signal is observed with a high contrast. Labeling with such probes do not alter virion morphology, integrity, nor infectivity. Finally, it is shown by fluorescence microscopy that these probes enable efficient tracking of labeled HCVpp inside hepatocarcinoma cells used as model hepatocytes, in spite of their autofluorescence up to 700 nm. These novel fluorescent lipid-polymer probes should therefore enable a better characterization of early stages of infection of autofluorescent cells by enveloped viruses.

W. Lacour, Dr. S. Adjili, Dr. A. Favier, Dr. K. Monier,
Dr. C. Place, Dr. M.-T. Charreyre
Université Lyon
Ens de Lyon
CNRS
Laboratoire Joliot-Curie
F-69342 Lyon, France
E-mail: marie-therese.charreyre@ens-lyon.fr
W. Lacour, Dr. S. Adjili, Dr. A. Favier, S. Mezhoud,
Dr. C. Ladavière, Dr. M.-T. Charreyre
Université Lyon
INSA Lyon
Université Claude Bernard
CNRS
Laboratoire Ingénierie des Matériaux Polymères
F-69621 Villeurbanne, France
Dr. J. Blaising,[+] Dr. E.-I. Pécheur
Université Lyon
Univ Claude Bernard
INSERM U1052
CNRS 5286
Centre de Recherche en Cancérologie de Lyon (CRCL)
F-69424 Lyon, France
E-mail: eve-isabelle.pecheur@inserm.fr
Dr. C. Place
Université Lyon
Ens de Lyon
Université Claude Bernard
CNRS
Laboratoire de Physique
F-69342 Lyon, France

[+]Present address: Roche Pharma Research and Early Development, Roche R&D Center, Shanghai, 201203, China

1. Introduction

In the context of recent severe outbreaks of potentially lethal viral infections (e.g., Ebola fever, avian flu, SARS), the control of globally prevalent infections caused by viruses of influenza, herpes, hepatitis or filoviruses such as Ebola should be a paramount and continuous consideration. Early stages of infection include the attachment of viral particles to host cell membranes, followed by virion internalization in intracellular compartments and release of the viral genome inside the cell. These stages are still badly characterized for several enveloped viruses.

Until recently, most observations of virions were performed by transmission electron microscopy (TEM) and more rarely by atomic force microscopy (AFM).[1] TEM provides exceptional resolution but requires tedious preparation steps. Samples must be fixed prior to observation, hampering any observation of viruses infecting live cells. AFM does not require a heavy preparation but does not enable to follow virions inside cells. However, the tracking of viral particles at various stages of their interactions with host cells is crucial to understand the infection mechanisms and undertake relevant antiviral therapies.

Herein, our first objective is to achieve a robust fluorescent labeling of enveloped virions. The chosen model is the hepatitis C virus (HCV, ≈100 nm diameter), for which only few fluorescent probes have been used to label its lipid envelope. Randall's group developed a strategy based on the use of a small lipophilic dye, DiD (1,1-dioctadecyl-3,3,3-tetramethyl-indodicarbocyanine). Its fluorescence is greatly enhanced when spontaneously inserting into membranes.[2] However, due to its small size, it is susceptible of release from the viral envelope with time, thereby leading to fluorescence signal dilution. Recently, Pécheur's group, developing strategies using octadecyl-Rhodamine B chloride (R_{18}), strengthened the observation that HCV enters hepatocytes by clathrin-dependent endocytosis and unraveled the mechanisms of action of two antiviral molecules.[3,4] However, the fluorescence signal of this *molecular* lipid probe is again rapidly diluted intracellularly, preventing the long-term tracking of labeled viral particles.

We previously designed various kinds of biomolecule-end-functionalized polymer chains (e.g., with biotin, saccharide, phospholipid),[5–7] including lipid-ended polymers able to interact with the lipid bilayer of artificial systems such as

Materials
Views
www.MaterialsViews.com

ADVANCED
HEALTHCARE
MATERIALS
www.advhealthmat.de

FULL PAPER

LipoParticles[8] and liposomes.[9] In the former case, a lipid-ended homopolymer provided steric stabilization to LipoParticles at high salt concentration; in the latter case, a fluorescent lipid-ended copolymer coud label liposomes of various sizes, giant (GUV), large (LUV), and small unilamellar vesicles (SUV), with diameters respectively around 5 µm, 100 nm, and below 100 nm. Such fluorescent lipid-polymer conjugates therefore appear most appropriate as *macromolecular* lipid probes to label enveloped viruses.

For an efficient fluorescent labeling, the probe should be bright, resistant to photobleaching, and provide a stable labeling with no (or limited) leakage from the viral membrane, to enable visualization during several minutes without loss of contrast. Additionally, insertion of the probe should alter neither the morphology, integrity, nor infectivity of the labeled virions.

Our second objective is to track by fluorescence microscopy labeled virions inside autofluorescent host cells, a phenomenon that complicates optical observations. Hepatocytes exhibit autofluorescence over the whole visible range, till ≈700 nm.[10] To circumvent this, we designed lipid-polymer probes emitting in the far-red range (650–750 nm) of major interest compared to the near-infrared one (NIR, 750–950 nm). Indeed, both far-red and NIR ranges enable to avoid most of the hepatocyte autofluorescence; however, observations in the NIR range require specific optics and camera.

Two far-red emitting fluorophores were chosen: (i) a commercially available water-soluble dye bearing three negative charges and displaying a large extinction coefficient, FluoProbes®647H (called "A" thereafter); (ii) an uncharged dye synthesized in Andraud's laboratory,[11] belonging to the isophorone family and displaying a large Stokes shift of high interest for microscopy[12] (called "B" thereafter). We previously showed that although B dye is hydrophobic, its binding onto hydrophilic polymers led to water-soluble probes, provided that the fluorophore density remained below 4 mol%.[9]

Here, we report (i) the synthesis of A-based lipid-polymer probe, followed by thorough optical characterization of both A- and B-based fluorescent lipid-polymer probes, (ii) their use for the labeling of a surrogate model of HCV, and (iii) observation of the resulting labeled virions inside their autofluorescent host cells, hepatocytes, by optical microscopy.

2. Results

2.1. Synthesis of the Far-Red Fluorescent Polymer Probes

The far-red fluorescent polymer probes were synthesized by covalent binding of far-red emitting fluorophores along water-soluble and biocompatible copolymer chains based on poly(*N*-acryloylmorpholine-*co*-*N*-acryloxysuccinimide), P(NAM-*co*-NAS). Our aim was to bind several fluorophores *per* chain to increase the brightness of the resulting probe, taking into account the solubility and the inherent self-quenching phenomenon. Polymer chains with/without a lipid end-group were labeled with either FluoProbes®647H (called "A") or an isophorone derivative (called "B").
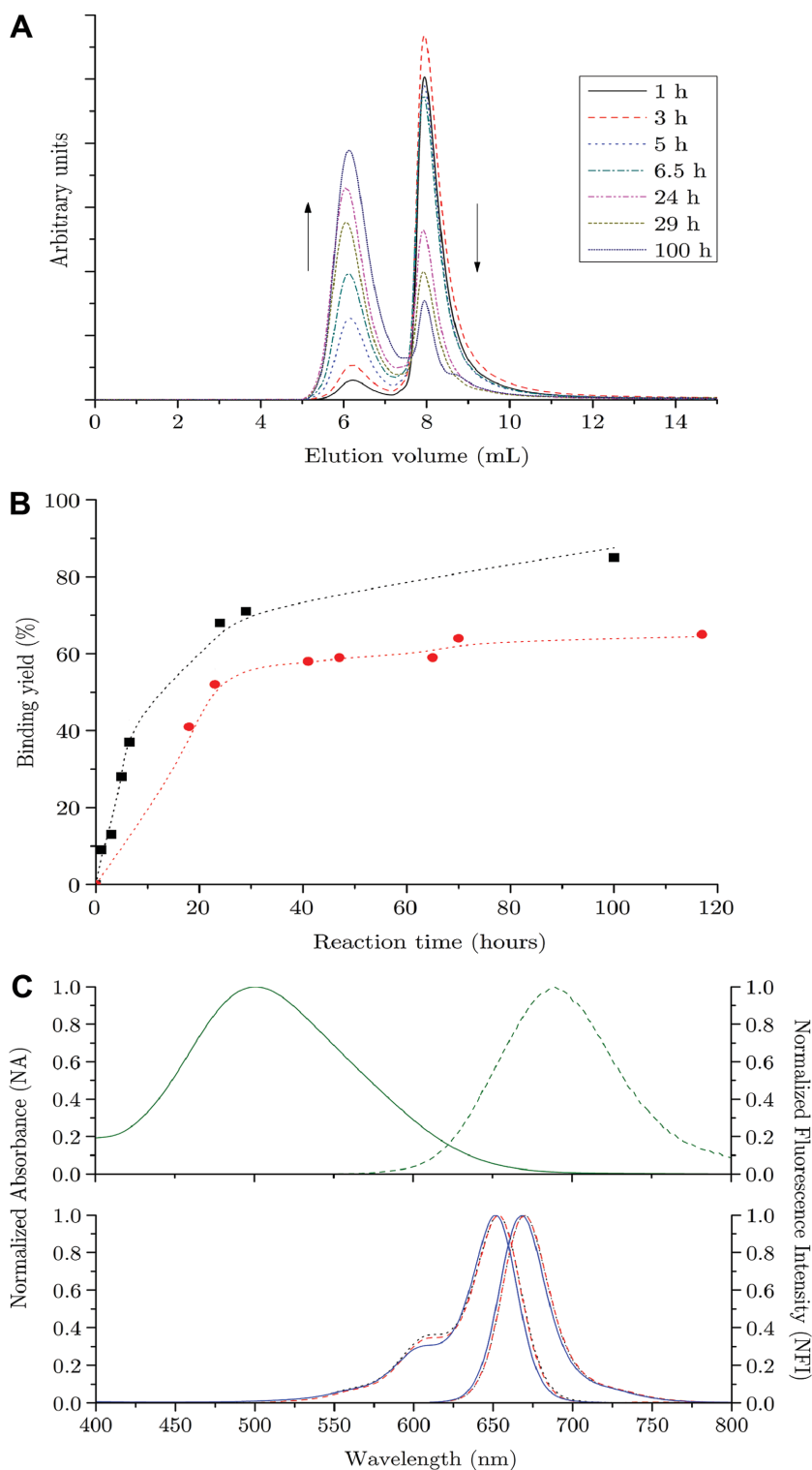
B dye binding was carried out as previously described.[9] Much effort was devoted to achieve the optimal conditions for the synthesis and purification of A-based polymer probes. The binding was performed in DMF, a solvent common to both polymer and dye (A was not soluble in chloroform). The binding reaction was monitored by SEC with a double refractometric/UV–vis detection, the bound dye appearing at a smaller elution volume (6.2 mL) than the free dye (8 mL) (**Figure 1**A). The ratio between the two peaks enabled determination of the binding yield. The reaction was slow but could be accelerated by a supplementary equivalent of DIPEA after 3 h. No further improvement occurred after addition of a third equivalent after 1 d (Figure 1B). The kinetics reached a plateau with a 86% binding yield after 4 d (**Table 1**). The difference between the binding yields of A onto lipid- or nonlipid-ended polymers (60% vs 86%, respectively), could be explained by a less favorable conformation of the chain in DMF due to the apolar character of the lipid end-group, rendering activated ester functions less accessible.

Residual-activated ester functions were hydrolyzed in situ, leading to negatively charged polymer backbones (carboxylate functions at pH 7). The presence of such a large number of carboxylate groups per chain was expected to further improve water-solubility and favor an extended conformation of the polymer chain due to electrostatic repulsions. Purification of A-based polymer probes was first attempted by dialysis against water (Figure S1, Supporting Information). However, surprisingly, the free dye although perfectly water-soluble did not cross the dialysis membrane regardless of its molecular weight cutoff (2000–15 000 g mol^{-1}). Finally, we could fully remove it by performing a dialysis against a 0.5 M NaCl solution (Figure S2, Supporting Information), followed by a dialysis against water to remove NaCl salt.

2.2. Photophysical Characterization of the Fluorescent Polymer Probes

Absorption and fluorescence emission spectra of A-based-polymer probes in water were similar to those of the free dye (Figure 1C, bottom) with no difference for probes harboring a lipid end-group. Optical characteristics of B-based-polymer probes could also be determined in water (contrary to those of B dye) thanks to the hydrophilic polymer chain (Figure 1C, top). A Stokes shift of 180 nm (5150 cm^{-1}) was recorded, even larger than that of the free dye in CHCl$_3$ (135 nm, 4180 cm^{-1}), mainly due to the redshift of the fluorescence emission from chloroform to water.[9] For both kinds of polymer probes, the fluorescence emission band was observed in the far-red region (650–750 nm).

The molar extinction coefficient (ε) and fluorescence quantum yield (Φ) of each polymer probe were determined from the absorption and emission spectra, respectively (**Table 2**). In all cases, ε values were much higher for polymer probes than for free dyes. Concerning Φ, it is generally expected to decrease when the local dye concentration increases, due to self-quenching.[13] This is indeed observed here, as the dye density along the polymer chain increases.[7] However, Φ value of the bound dye still represents 66%–76%

FULL PAPER

**ADVANCED
HEALTHCARE
MATERIALS**
www.advhealthmat.de

*Materials
Views*
www.MaterialsViews.com

Figure 1. A) Evolution of the reaction media (19K4H-A) followed by size exclusion chromatography (UV–vis detector at 650 nm; 6.2 mL: bound dye; 8 mL: free dye). B) Binding kinetics of A dye along a polymer chain with (L-20K3H-A, red circles) and without (19K4H-A, black squares) lipid end-group. C) Absorption and fluorescence emission spectra in water of (bottom): A-based-polymer probes, 19K4H-A (black dotted line) and L-20K3H-A (red dashed line), superimposed with free A dye (blue full line) and compared to (top): B-based-polymer probe 34K9H-B.

of the free dye one, reflecting a positive influence of the carboxylate groups along the chain that favor an extended conformation of the polymer chain due to electrostatic repulsions, thereby limiting the occurrence of dimer formation (usually nonfluorescent). Finally, a binding of 3 to 9 fluorophores per chain provided in all cases water-soluble polymer probes with limited self-quenching. The brightness of the polymer probes was determined from their ε and Φ values, and was found two to fivefold higher than that of free fluorophores.

2.3. Labeling of Artificial Lipid Bilayers (LipoParticles) by Fluorescent Polymer Probes

LipoParticles emerged as promising entities for biotechnological applications, ranging from model membrane systems or biomolecule screening supports to therapeutic vectors.[14] Their versatile structure is due to the possibility of varying particle nature/size and lipid formulation.[30,31] Among all kinds of reported LipoParticles, those with sizes equal to or above 1 µm are the most relevant for optical observations. We therefore decided to use such LipoParticles as artificial lipid bilayers mimicking viral envelopes, to evaluate the anchoring properties of our fluorescent lipid-polymer probes. Two strategies were chosen (**Figure 2**A): (1) incorporation of the probes during the preparation process of liposomes, further mixed with micrometer-sized polystyrene particles in specific conditions leading to their reorganization onto the colloidal surface; (2) "simple contact" between preformed LipoParticles and probes. For both strategies, LipoParticles appeared as individualized and localized fluorescent dots. Comparison of bright field and fluorescence microscopy images clearly showed that almost all particles were labeled by the probe (Figure 2B).

2.4. Labeling of Enveloped Viral Particles by the Fluorescent Polymer Probes

The use of a new fluorescent probe to label a biological entity requires a thorough investigation of its potential cytotoxicity and resistance to photobleaching. Previous cytotoxicity studies on several B-based-polymer probes had revealed no toxicity up to 10×10^{-6} M on human adherent (HeLa) and nonadherent (T lymphocytes) cells.[15] Moreover,

Makrials
Views
www.MaterialsViews.com

ADVANCED
HEALTHCARE
MATERIALS
www.advhealthmat.de

FULL PAPER

Table 1. Physico-chemical characteristics of the far-red fluorescent polymer probes.

Polymer probe sample		M_n of polymer backbone g.mol^{-1} (Đ)[a]	Fluorophore binding yield[b]	Average number of fluorophores per polymer chain[b]	Maximum number of charges per polymer chain[c]	Average fluorophore density[d] %
L-20K3H-A		20 300 (1.04)	60%	3.0	59	2.3
19K4H-A		19 400 (1.07)	86%	4.3	60	3.4
L-20K4H-B		20 300 (1.04)	60%	3.8	47	3.0
34K9H-B		34 200 (1.10)	66%	8.5	78	3.9

[a]Dispersity, representative of the polymer chain size distribution; [b]determined by SEC with a UV–vis detector; [c]the charges along the polymer backbone arise from the dye (3 negative charges per A dye) and/or from a variable number of deprotonated -COOH groups depending on the pH and on the distribution of these groups along the polymer chain; [d]number of fluorophores related to the total monomer units per polymer chain.

B-based-polymer probes have been evaluated with success for in vivo labeling of zebrafish embryos, with no significant lethality nor abnormality or delayed development.[15] In addition, they appeared more resistant to photobleaching than a commercial far-red-emitting molecular probe, LysoTracker Red DND-99.[15] A-based-polymer probes exhibited no cytotoxicity on hepatocarcinoma Huh7.5 cells for concentrations up to 1×10^{-6} M (data not shown). They also greatly resisted to photobleaching, since even under forced conditions (constant illumination at 100% light source power, whereas 25% is generally used for imaging), it was possible to record more than 40 successive images in cellulo before significant photobleaching occurred (Figure S3, Supporting Information). Such proper-
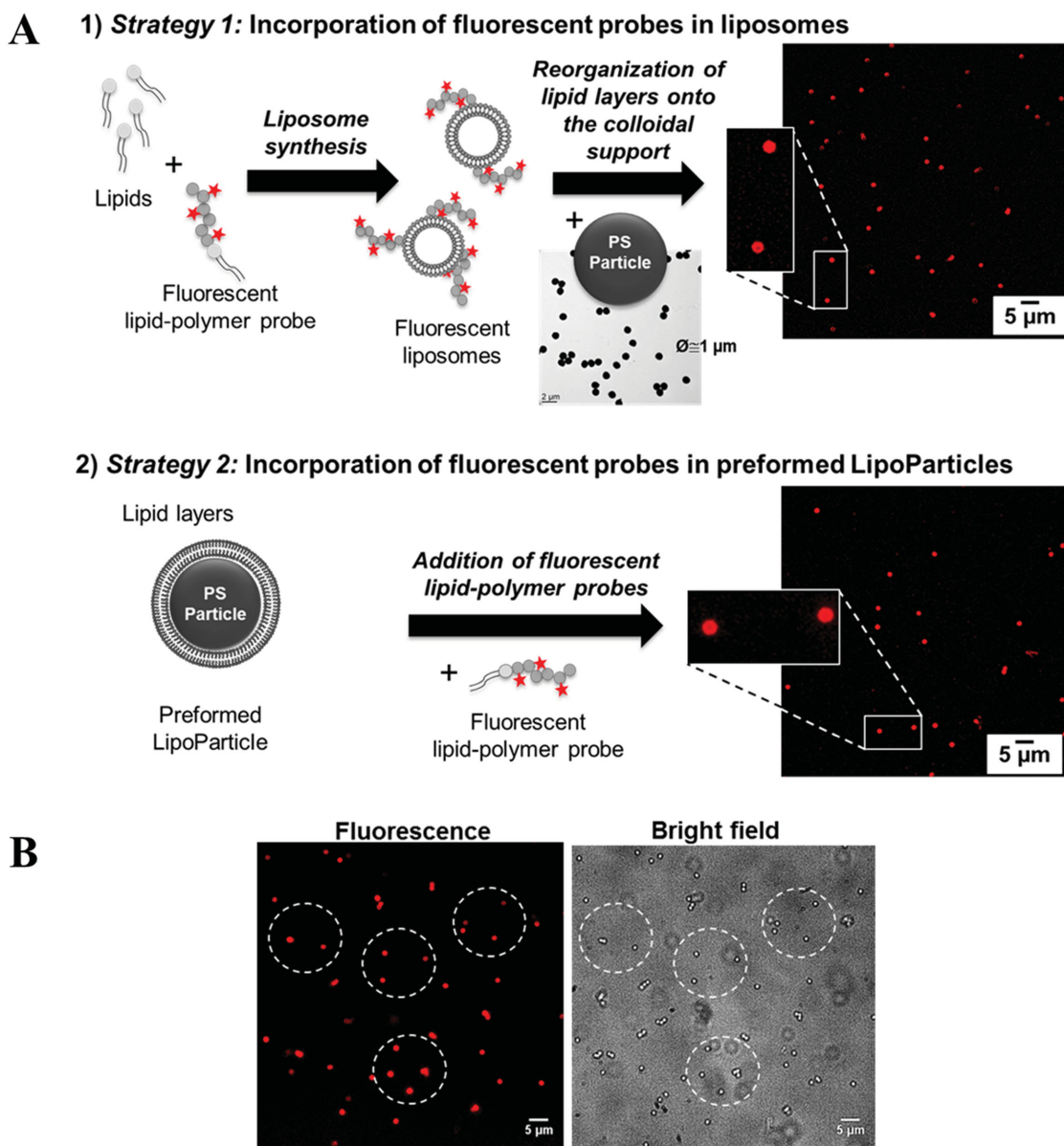
ties were therefore favorable to undertake enveloped virion labeling.

Handling infectious viruses is a tedious procedure which can include production and purification steps in Biosafety Level 3 laboratories, with random yields in terms of infectivity and purity of the final viral samples. In order to bypass such limitations, we used a surrogate model of HCV virions, that is, pseudotyped particles (HCVpp). They are easy to produce in cell cultures, at high rates and with optimal reproducibility between batches.[35] HCVpp are assembled onto a retroviral core, harbor the viral glycoproteins E1-E2 at their surface (embedded in the lipid envelope), and are most suitable to track viral entry events.[3,4]

Table 2. Photophysical characteristics of the far-red fluorescent polymer probes in water.

Probe sample		λ_{abs} [max/nm]	λ_{em} [max/nm]	$\varepsilon\ [\lambda_{abs\ max}]$[a] [M^{-1}.cm^{-1}]	Fluorescence quantum yield Φ	Relative brightness[b]
A-free dye		651	670	192 000 ± 10,000	—	1
L-20K3H-A		653	668	345 000 ± 14,000	0.89[c]	1.9
19K4H-A		653	669	680 000 ± 20,000	0.76[c]	2.4
B-free dye[d]		505	640	19 000 ± 5000	0.07 ± 0.02[e]	1
L-20K4H-B		508	688	60 000 ± 10,000	0.08 ± 0.02[e]	3.5
34K9H-B		501	679	137 000 ± 5000	0.05 ± 0.01[e]	4.8

[a]Determined taking into account the -COONa form in the M_n calculation of the polymer chain; [b]brightness ($\varepsilon.\Phi$) of the polymer probe relative to free dye brightness; [c]relative fluorescence quantum yield (to free A dye); [d]values determined in CHCl$_3$ since free B dye is not soluble in water; [e]determined at $\lambda_{Ex} = 510$ nm using Erythrosin-B in MeOH ($\Phi = 0.09$) as reference.[29]

**ADVANCED
HEALTHCARE
MATERIALS**

www.advhealthmat.de

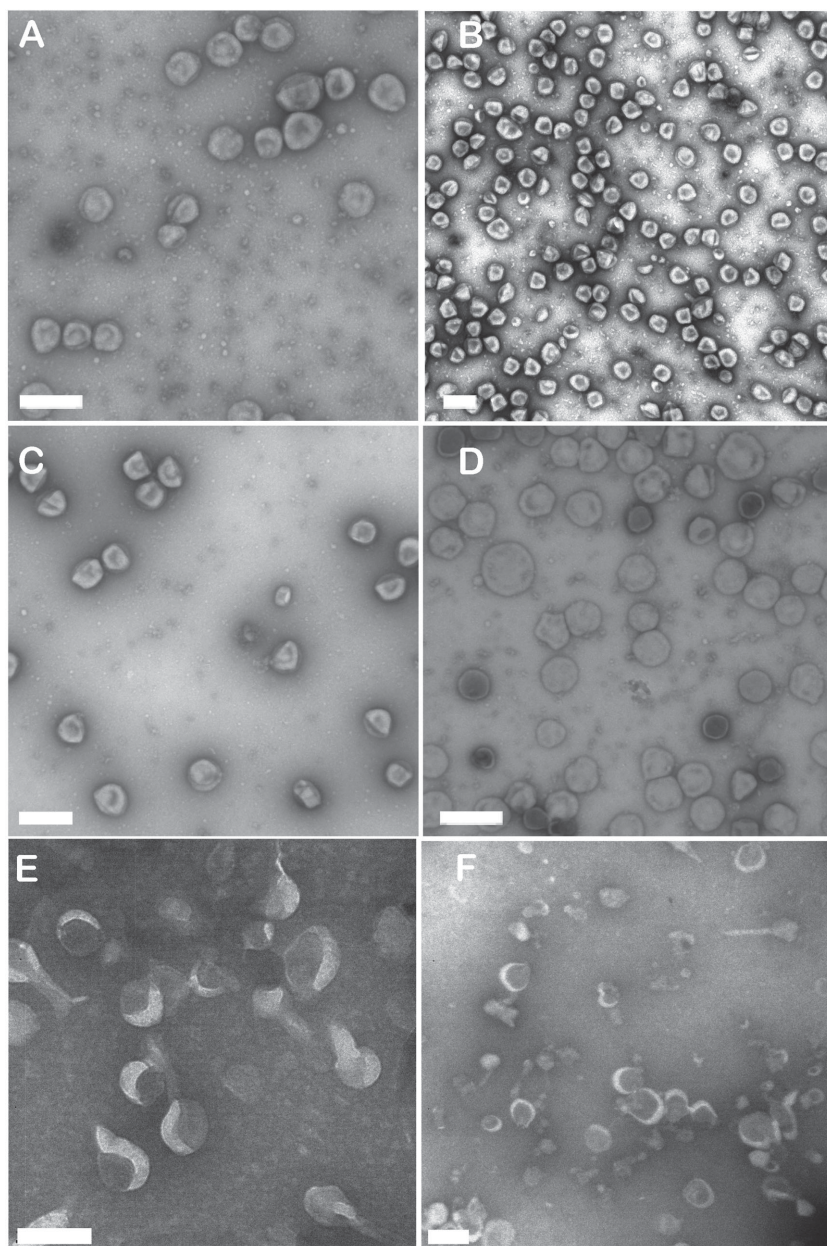**Materials
Views**

www.MaterialsViews.com

FULL PAPER

Figure 2. A) Two strategies to incorporate the fluorescent lipid-polymer probe L-20K4H-B in LipoParticles. (1) Fluorescent liposomes mixed with polystyrene particles (TEM image). (2) Probe mixed with preformed LipoParticles. Fluorescence microscopy images are shown on the right (insets: 2 zooms of species). B) For strategy 1, corresponding fluorescence (left) and bright field (right) microscopy images (white circles are a guide to the eyes).

HCVpp were labeled in parallel with both kinds of fluorescent lipid-polymer probes (bearing either A or B dye). They were also labeled with the corresponding probes without lipid end-group, in order to assess the influence of the lipid moiety. As an additional control, we used DiD as a commercial molecular lipid probe. The same procedure was used for the five probes, and labeled HCVpp were subsequently purified.[3] Handling of the lipid-polymer probes and their subsequent use for HCVpp labeling were greatly facilitated by their water-solubility. Most importantly, these aqueous solutions are stable for months when stored at 4 °C away for light; indeed a batch of probes synthesized in 2012 exhibited similar labeling and fluorescence properties when used in 2015.

2.5. Observation of Labeled HCVpp by TEM

TEM imaging was carried out to check at the nanometric scale the integrity and morphology of labeled HCVpp. Uranyle acetate was chosen as the negative stain; however, in spite of numerous attempts, in the case of B-based probes, the use of uranyle acetate induced morphological artifacts to the labeled particles; we therefore chose to use phosphotungstic acid as a contrast agent instead (**Figure 3**E,F; Figure S4, Supporting Information). As shown in Figure 3 and Figure S4, particles labeled with A- or B-based-polymer probes with or without lipid end-group, maintained a similar morphology as that of unlabeled HCVpp, with neither particle aggregation nor

Figure 3. TEM images of HCVpp after negative staining with uranyle acetate (A–D) or phosphotungstic acid (E,F). Unlabeled A), labeled with DiD B), with A-based polymer probe without C) or with D) lipid end-group, with B-based polymer probe without E) or with F) lipid end-group (scale bar 0.2 µm).

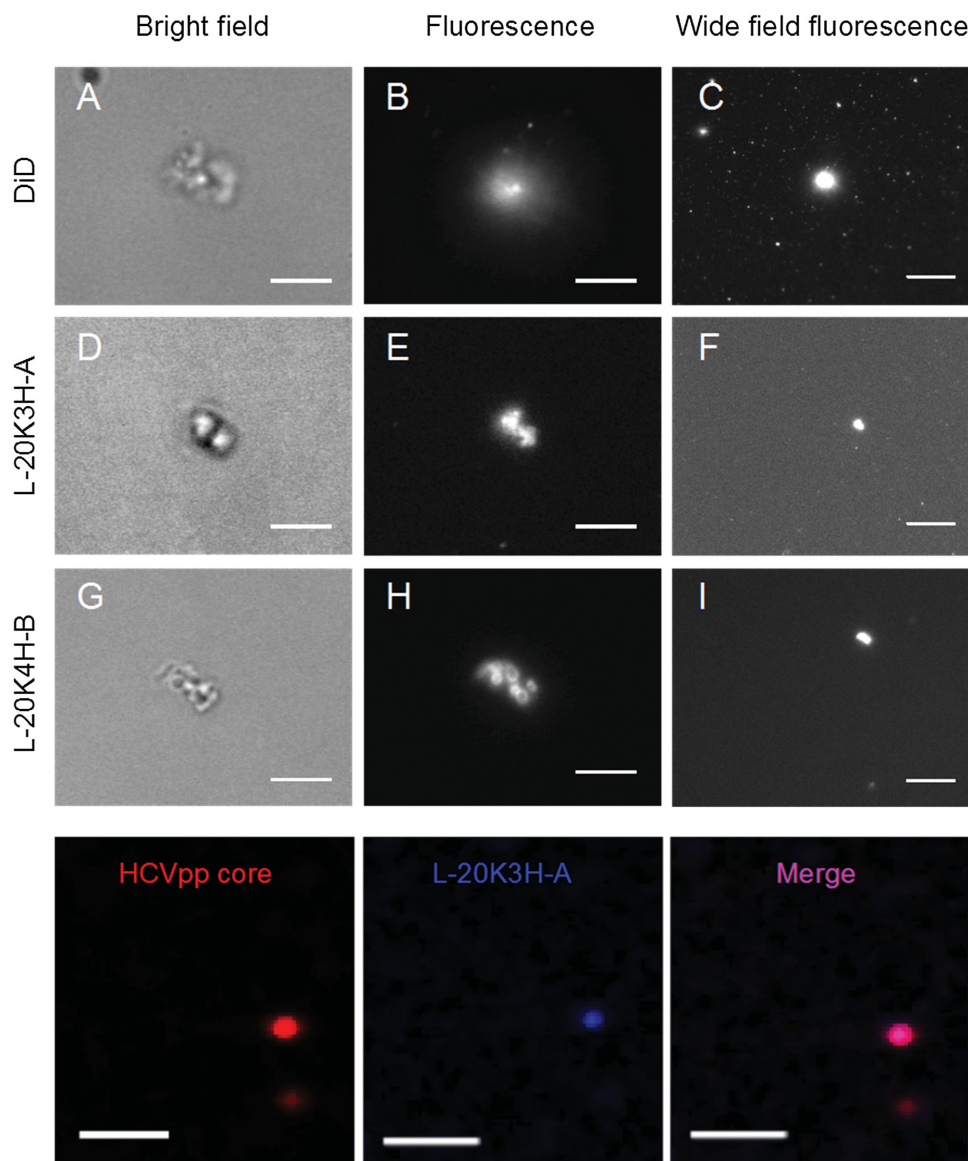A- or B-based-probes? and (iv) lipid-ended or nonlipid-ended probes?

First, enlarged images (×4) from bright field and fluorescence microscopy (**Figure 4**, top panels) showed micrometer-sized clusters of HCVpp (Figure 4A,D,G). These clusters appeared strongly fluorescent with a very high contrast, indicating that HCVpp labeling with both kinds of lipid-polymer probes was at least as bright as that with DiD (Figure 4E,H compared to B). The corresponding wide field images showed many fluorescent small spots in the case of DiD labeling (Figure 4C). In contrast, such fluorescent small spots were not observed in the case of labeling with each lipid-polymer probe (Figure 4F,I), indicating a more stable labeling of HCVpp with lipid-polymer probes than with DiD.

Additionally, we performed indirect immunofluorescence to label the retroviral nucleocapsid of HCVpp, to ascertain the specificity of our lipid labeling for entire virions and not for empty viral particles or membrane debris. It revealed that the signal of HCVpp Gag retroviral core[35] colocalized with the lipid-polymer probe signal (Figure 4, bottom panels), confirming that the fluorescent clusters corresponded to entire virions.

Finally, labeling with lipid-ended or nonlipid-ended polymer probes was compared (**Figure 5**). When nonlipid-ended polymer probes were used, HCVpp clusters were not fluorescent (Figure 5D,H), conversely to those labeled with lipid-ended probes (Figure 5B,F). This was reproducible and comparable for A- and B-based polymer probes, strongly underlining that the presence of the lipid end-group in the polymer probe architecture is crucial for an efficient labeling of enveloped virions.

2.7. Infectivity of Labeled HCVpp and Observations after Infection of Hepatocarcinoma Huh7.5 Cells

After virion labeling with a probe, subsequent infectivity must be assessed (**Figure 6**A). As reported,[35] HCVpp infectivity was enhanced after their 100-fold concentration from cell supernatant (compare second with third bars). Importantly, probe-labeled concentrated HCVpp only displayed a 15 to 20% loss of infectivity after purification, as compared with unlabeled concentrated HCVpp. Therefore, polymer probe incorporation per se only marginally alters HCVpp infectivity. A comparable result was obtained with DiD-labeled HCVpp, in line with our previous results[4] with R_{18}. Noteworthy, infectivity of HCVpp that had been in contact with nonlipid-ended polymer probes was comparable
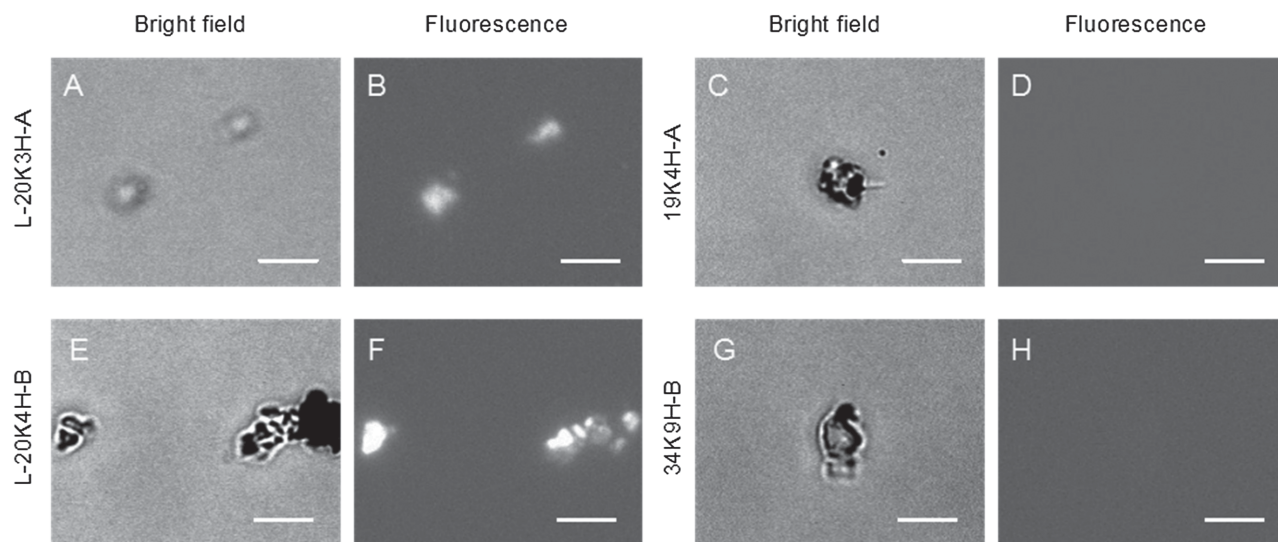
lysis. The DiD probe also did not alter particle integrity nor morphology.

2.6. Observation of Labeled HCVpp by Bright Field and Fluorescence Microscopy

Next, we sought to answer the following questions: (i) are the polymer probes capable of labeling enveloped virions? (ii) if so, is this labeling comparable or better than that achieved with DiD? Is there a difference between (iii) labeling achieved with

Figure 4. Top panels: bright field (A,D,G, scale bar 5 µm), fluorescence (B,E,H, scale bar 5 µm), and wide field fluorescence (C,F,I, scale bar 20 µm) microscopy images of HCVpp labeled by DiD probe (A,B,C, λ_{Em} = 670 nm) or by the far-red lipid-polymer probes based either on A dye (D,E,F, λ_{Em} = 670 nm) or B dye (G,H,I, λ_{Em} = 690 nm) (objective lens 63×). Bottom panels: Representative confocal images of HCVpp immuno-stained for Gag retroviral core protein (left, red) and labeled with L-20K3H-A (middle, presented as a false blue color) with the merge (right, magenta) (bar 5 µm).

to that of unlabeled HCVpp, confirming the safety of our probes.

We next examined whether the fluorescence emission of the polymer probes in the far-red range was favorable to the observation of labeled HCVpp inside hepatocytes, commonly known to be autofluorescent (due to the presence of porphyrins[16] and copper-metallothionein complexes[17] in their intracellular compartments). Since hepatocarcinoma cells were reported to display a bright red-orange autofluorescence,[18] we first investigated the fluorescence properties of human hepatocarcinoma Huh7.5 cells over the UV, visible and far-red wavelength range. They exhibited a strong autofluorescence in all ranges, except in the far-red where autofluorescence was very low (Figure S5,

Supporting Information). Importantly, it was not dependent upon the use of a fixative agent. This observation strengthened our assumption that the use of far-red fluorescent probes would enable efficient tracking of virions inside cells displaying autofluorescence.

We infected Huh7.5 cells with HCVpp labeled or not with L-20K3H-A (Figure 6B). A very low fluorescence intensity was observed with unlabeled HCVpp (panel b) reflecting the detection of cell autofluorescence in the Cy5 channel (Em 725 nm/75 nm). Conversely, after only a 10 min-contact between labeled HCVpp and Huh7.5 cells at 37 °C, highly fluorescent spherical dots were visible (diameter close to 1 µm, panel e) randomly distributed in the cytoplasm (panel f). This was

Materials Views
www.MaterialsViews.com

ADVANCED
HEALTHCARE
MATERIALS
www.advhealthmat.de

FULL PAPER

Figure 5. (A,C,E,G) Bright field and (B, D, F, H) fluorescence microscopy images of HCVpp labeled by the polymer probes either with lipid end-group (L-20K3H-A: A,B, and L-20K4H-B: E,F) or without lipid end-group (19K4H-A: C,D, and 34K9H-B: G, H) (objective lens 63×, scale bar 5 µm).

comparable to previous observations with DiD or R_{18} probes.[2,4] After a 30 min-contact (panel h), these highly fluorescent dots had migrated further inside the cells, closer to the nucleus (panel i), in agreement with previous reports on HCV intracellular trafficking.[3,4]

To ascertain that the highly fluorescent spherical dots observed intracellularly corresponded to clusters of labeled HCVpp, we performed colocalization experiments after Gag immuno-staining. For these experiments, cells were also stained for clathrin, a main protein actor of HCV internalization through endocytosis.[4,19] Cells were successively imaged at 488 nm (green, to reveal clathrin), 594 nm (red, to reveal HCVpp Gag), and 635 nm (false blue color, to reveal L-20K3H-A polymer probe labeling of HCVpp envelope).

Gag fluorescence signal perfectly colocalized with that of L-20K3H-A probe (**Figure 7**, merge = magenta dots), once again confirming the labeling of viral particles by the polymer probe. This fluorescence signal was distributed throughout the cell after 10 min contact at 37 °C (Figure 7A) and gathered at the periphery of the nucleus after 30 min (Figure 7B), in line with data shown above (Figure 6B). Interestingly, L-20K3H-A-labeled HCVpp were detected in clathrin-coated vesicles resulting in white dots (Figure 7B, asterisks in zoom). This indicates that L-20K3H-A-labeled HCVpp are internalized by hepatocytes through clathrin-dependent endocytosis, in complete agreement with literature on HCV cell entry, and thereby confirming at the cellular level that labeling of viral particles by the lipid-polymer probes does not alter their biological properties.

2.8. Discussion

The life cycles of several viruses of medical importance are still poorly understood; this considerably hampers our possibilities to define appropriate therapeutic targets and design efficient antivirals. Unraveling the ways they infect their host cells at

the molecular level is therefore of paramount importance, especially entry pathways.

Our aim was to design novel fluorescent lipid probes capable of robust labeling of enveloped viruses to track them in autofluorescent cells by optical microscopy. For this purpose, probes based on a biocompatible polymer backbone presenting a phospholipid moiety at one chain-end and multiple fluorophores along the chain were synthesized (**Figure 8**). Two kinds of dyes were used: a commercial one displaying a high extinction coefficient, FluoProbes®647H, and an isophorone derivative displaying a large Stokes shift.[11] The resulting polymer probes exhibited similar absorption and emission spectra as the free dye, with a fluorescence emission in the far-red range (Figure 1). An optimized binding of the dyes provided water-soluble polymer probes with a two- to fivefold brightness increase in comparison with the corresponding free dyes (Tables 1 and 2). Such lipid-polymer probes successfully labeled artificial lipid bilayers (Figure 2).

HCV was chosen as a model enveloped virus, since early steps of its entry into hepatocytes have been described,[20] thereby facilitating establishment of a proof-of-concept using our new probes to label virions. Yet, several stages of its interactions with host cells remain ill-defined, and most importantly, hepatocytes are autofluorescent cells, which precludes the use of probes emitting in the visible range for observations by optical microscopy.[16–18] Labeling of a surrogate model of HCV, HCV pseudoparticles (HCVpp), with our far-red lipid-polymer probes was more stable and reproducible than using a commercial probe (Figure 4). As a direct consequence, a strong fluorescence signal was observed with a very high contrast, enabling visualization of virions for several minutes without loss of contrast. A complementary immunofluorescence assay confirmed the specificity of virion labeling, that is, observed particles consisted in fully enveloped virions containing a capsid. The only discriminating parameter was the presence of the lipid end-group in the polymer probe architecture
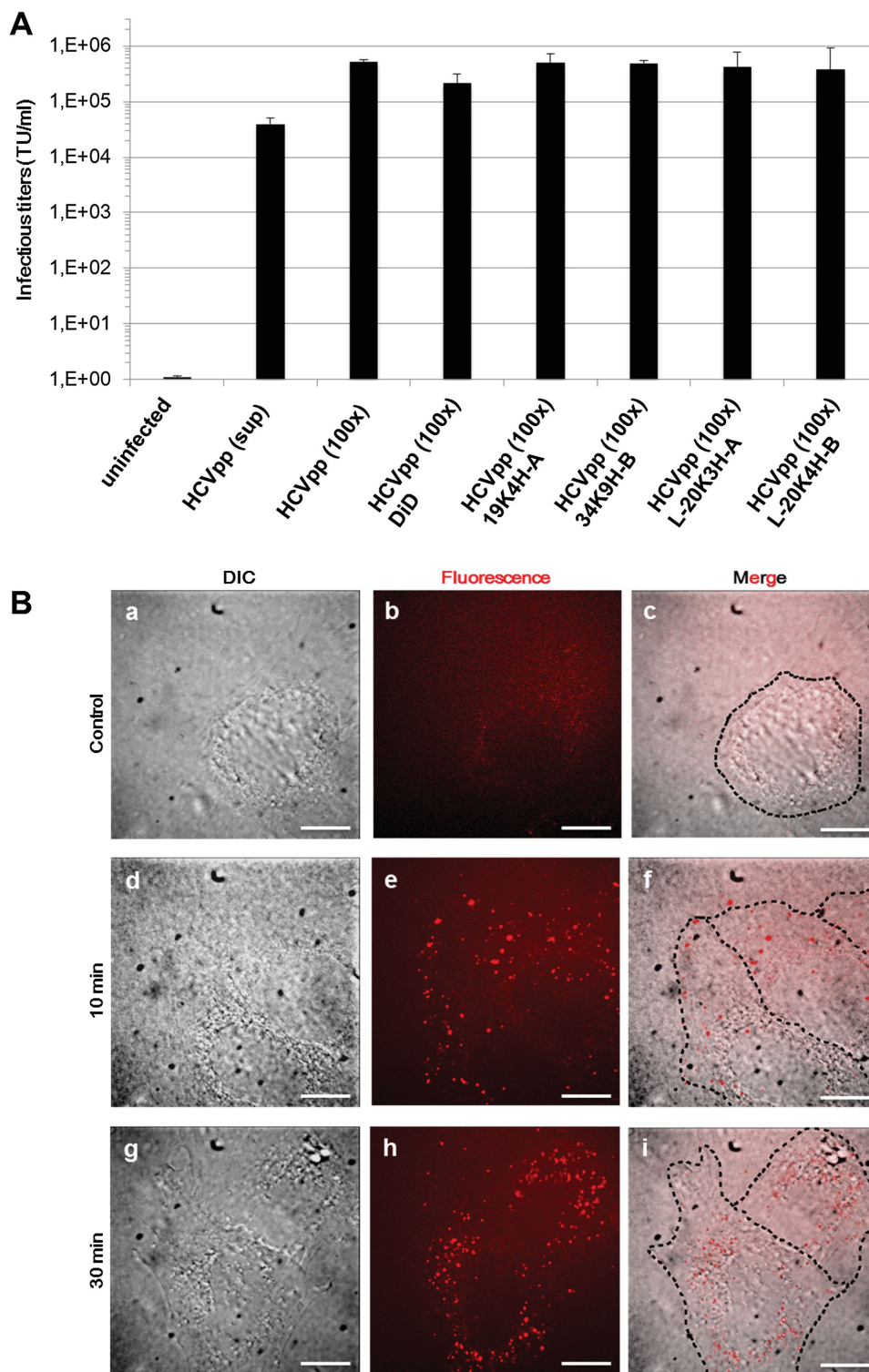
Figure 6. A) Infectivity test of HCVpp, as determined on Huh7.5 hepatocarcinoma cells. Results are displayed as TU per milliliter of supernatant (mean ± SD of two experiments). From left to right: uninfected cells; supernatants containing unlabeled HCVpp; unlabeled HCVpp concentrated 100× by ultracentrifugation; concentrated HCVpp labeled with DiD, 19K4H-A, 34K9H-B, L-20K3H-A and L-20K4H-B. B) Spinning-disk confocal microscopy projections (10 sections) of Huh7.5 cells, observed in Differential Interference Contrast (DIC, a,d,g) or in fluorescence (b,e,h), after infection with concentrated HCVpp, either unlabeled (a–c) or labeled with A-based-lipid-polymer probe L-20K3H-A, after 10 min (d–f) or 30 min (g–i) contact at 37 °C before cell fixation (100× oil immersion objective lens, bar 10 μm). Merged views (c,f,i) show intracellular distribution of labeled HCVpp. Dashed lines allow for cell contour visualization.

www.MaterialsViews.com

ADVANCED
HEALTHCARE
MATERIALS
www.advhealthmat.de

FULL PAPER
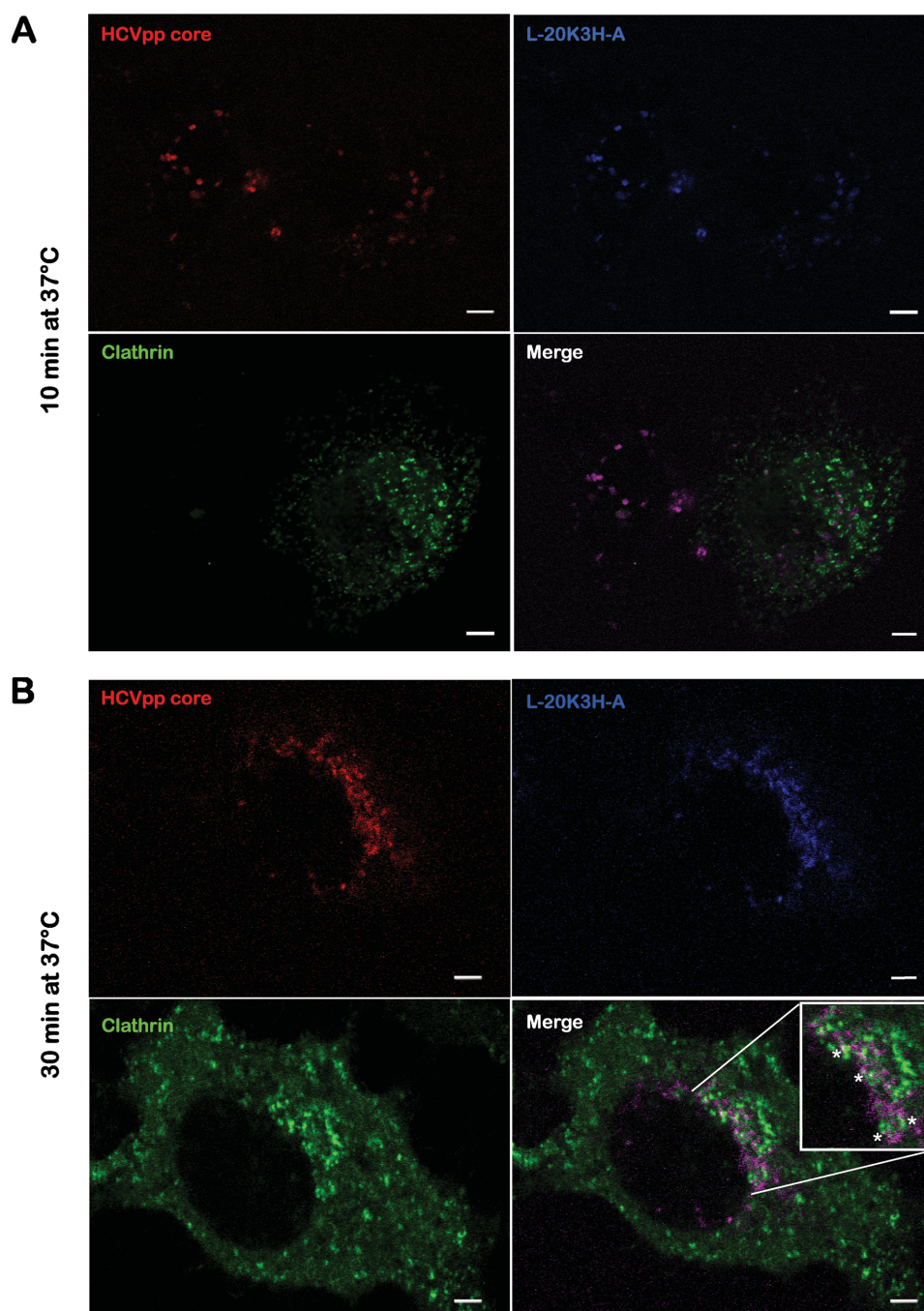
Figure 7. Representative confocal images of Huh7.5 cells infected with HCVpp labeled with L-20K3H-A, after a 10 min A) or 30 min contact B) at 37 °C before cell fixation (scale bar 5 μm). Cells were immuno-stained for Gag (HCVpp retroviral core protein, red) and for clathrin (as a marker of endocytosis, green). L-20K3H-A fluorescence is presented as a false blue color. Inset: zoom of selected cellular area; asterisks denote HCVpp fluorescence signals merging with clathrin (red + blue + green).

(Figure 5). In addition, labeling with the polymer probes did not alter the morphology nor the integrity of pseudotyped virions (Figure 3), and minimally affected their infectivity (Figure 6A). This strongly contrasts with the 200-fold loss of infectivity of HCV labeled with DiD, as observed by Randall and co-workers.[2] We confirmed that our labeling strategy did not alter the biological properties of virions, since they appeared to be internalized by clathrin-dependent endocytosis, as previously reported (Figure 7).[2–4]

Recent labeling strategies were based upon the coupling of quantum dots (QD) to the chemically modified surface of virions.[21,22] Although QD are highly bright and although virions were shown to retain their infectivity, the cytotoxicity of QD per se was not evaluated, while they appear to be cytotoxic
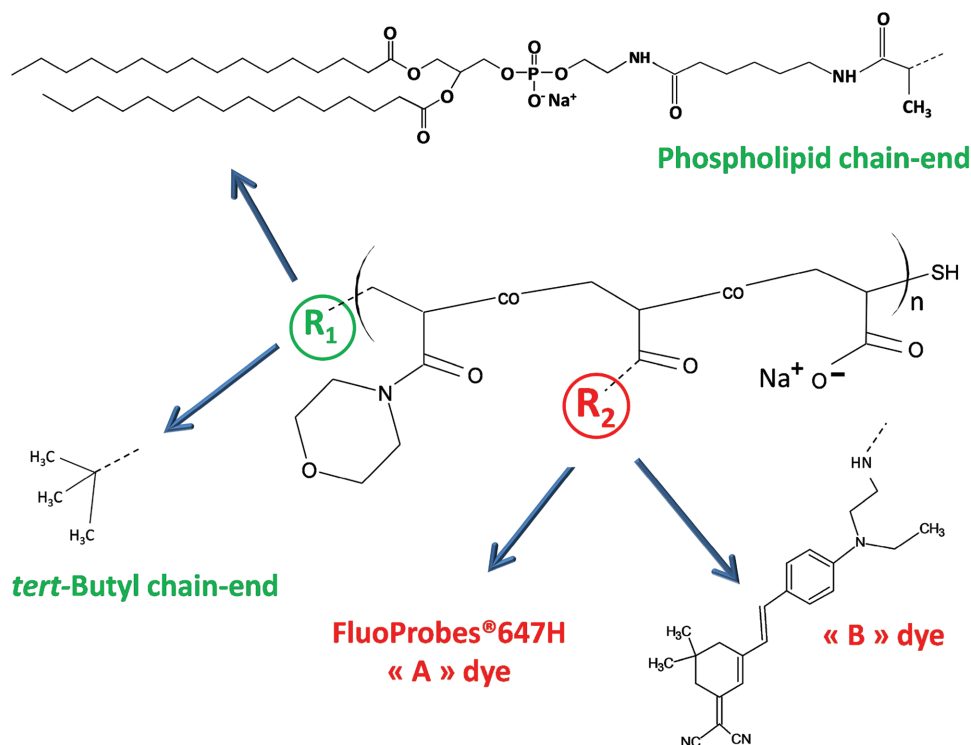
Figure 8. Chemical structure of the far-red fluorescent polymer probes (R_1 = end-group; R_2 = lateral group).

especially to hepatocytic cells.[23] Moreover, the overall size of QD conjugates (15–20 nm diameter) and the modification of viral surface might hamper the biological properties of labeled virions. Another strategy based upon the metabolic labeling of enveloped virions by azido sugars during infection was successfully developed.[24] However, it modifies the glycosylation profile of envelope glycoproteins, with the risk of altering their functional properties. By comparison, our small size biocompatible polymer probes (<10 nm) appear as safe means to label virions.

Using our far-red fluorescent lipid-polymer probes, we could achieve an efficient tracking of virions inside hepatocytic cells, with no optical contamination due to their autofluorescence up to 700 nm (Figure 6B and Figure 7). Several cell types are autofluorescent, which could lead to false-positive staining and erroneous conclusions.[25]

3. Conclusions

It appears that our novel far-red fluorescent lipid-polymer conjugates are most adequate probes to label enveloped viruses such as HCV (our study), and especially to perform intracellular tracking of labeled virions by optical microscopy at early stages of infection of autofluorescent cells. This proof-of-concept opens the way to the fluorescent labeling of other enveloped viruses, for example, influenza viruses, human herpes viruses, coronaviruses or filoviruses such as Ebola, which should lead to a better understanding of the infection mechanisms of these major human pathogens, in order to undertake relevant antiviral therapies.

4. Experimental Section

Materials: All chemicals were purchased from Sigma-Aldrich, Acros and Fluka at the highest purity available and used without further purification. Solvents were used as received from Fisher Scientific. Lipid dipalmitoylphosphoethanolamine (DPPE) was purchased from Avanti Polar Lipids. The FluoProbes®647H-amine dye ("A") was purchased from Interchim. The isophorone derivative dye ("B") has already been described.[11] Lipid-P(NAM-*co*-NAS) and P(NAM-*co*-NAS) copolymer chains have been previously synthesized, respectively from a lipid RAFT agent[9] and a *tert*-butyl dithiobenzoate RAFT agent.[26] All solvents used for the determination of photophysical properties were of spectrophotometric grade. Rabbit polyclonal antibody to human clathrin was from Abcam. The mouse monoclonal antibody to Gag retroviral core of HCVpp has been described elsewhere.[27] Dylight 488 and Dylight 594 secondary antibodies were from Pierce; their specificities for rabbit and mouse antibodies, respectively, were confirmed in each staining experiment.

Synthesis of the Polymer Probes: The synthesis of A-based-polymer probes was performed as follows: 20 mg (0.98 mmol of polymer chains corresponding to 52.2 mmol of NAS units) of P(NAM-*co*-NAS) copolymer (with or without a lipid end-group) were dissolved in 0.25 mL of dimethylformamide (DMF) in a 2 mL eppendorf tube. Dye A (5 mg, 5.4 mmol), dissolved in a 10/90:Vol/Vol water/DMF mixture) was added together with 2 molar equivalents of di-isopropylethylamine (DIPEA). Polymer concentration was adjusted to 20 mg mL^{-1} with DMF. The reaction was carried out at 40 °C in the dark under stirring for several hours. The binding yield was followed by size exclusion chromatography (SEC).

Hydrolysis of the residual activated ester units was carried out using 10 mL of borate buffer (50×10^{-3} M, pH = 9) directly added to the polymer solution at room temperature under stirring for 48 h. Then, conjugates were purified by dialysis (Spectrum Labs, Spectra/Por 7, MWCO: 15000 g mol^{-1}), first against a 0.5 M NaCl solution (2 baths), then deionized water (4 baths), and milliQ water (2 baths). The cyan-blue-colored A-based-polymer conjugates were dried by lyophilization.

www.MaterialsViews.com

www.advhealthmat.de

ADVANCED
HEALTHCARE
MATERIALS

FULL PAPER

The synthesis of B-based-polymer probes was carried out as published.[9]

Characterization Techniques: Size exclusion chromatography (SEC) with a UV–visible detector was used to monitor the binding yield of the fluorophore onto the P(NAM-*co*-NAS) copolymers following a previously described method.[28] This was performed using a Waters 1515 isocratic HPLC pump (flow rate: 1 mL min⁻¹) and a Styragel HR4E Waters column (7.8 × 300 mm²). The eluent was dimethylformamide (DMF) with LiBr (0.05 mol L⁻¹) at 30 °C. Detection was provided by both a Waters 2410 refractive index detector and a Waters 2489 UV–visible detector set at 488 nm (B dye) or 650 nm (A dye). Analyses were performed by injection of 10 µL of the reaction medium (diluted with DMF to 5 mg mL⁻¹). Data acquisition and treatment was performed using the Breeze software.

UV–visible absorption spectra were recorded on a Jasco V-670 spectrophotometer at ambient temperature using 1 cm quartz cells.

Fluorescence emission spectra were recorded on a Horiba–Jobin Yvon Fluorolog-3 spectrofluorimeter at 298K, using 1 cm quartz cells. The steady-state luminescence of diluted solutions was excited by unpolarized light from a 450 W xenon CW lamp and detected at right angle (90°) by a red-sensitive Hamamatsu R928 photomultiplier tube. Spectra were reference-corrected for both the excitation source light intensity variation (lamp and grating) and the emission spectral response (detector and grating). For A-based-polymer probes, reference was A dye itself at 600 nm excitation. For B-based-polymer probes, reference was Erythrosin-B in MeOH (Φ = 0.09) at 510 nm excitation.[29] Excitation of reference and sample was performed at the same wavelength.

Labeling of Artificial Lipid Bilayers (LipoParticles) with the Fluorescent Polymer Probes: The procedure to synthesize LipoParticles has been previously described.[30] Briefly, LipoParticles were prepared by adding preformed liposome dispersion to polystyrene particles. The mixture was vortexed for 1h at 70 °C and 1300 rpm. Thereafter, in order to separate the LipoParticles from nonadsorbed lipids, the dispersion was centrifuged at 9000×g for 10 min at 21 °C. The pellet containing LipoParticles was redispersed in pure water.

Preformed liposomes were prepared via a "hydration of a thin lipid film" process, the so-called Bangham method. Homogenization of size was performed by well-known sonication[30] or extrusion treatments.[31] For "Strategy 1," the lipid molar formulation used was 89/10/1 of 1,2-dipalmitoyl-*sn*-glycero-3-phosphocholine/1,2-dipalmitoyl-*sn*-glycero-3-phosphate/fluorescent lipid-polymer probe (DPPC/DPPA/L-20K4H-B). For "Strategy 2," the LipoParticles (prepared with 100% DPPC) were mixed with a solution of L-20K4H-B probe in water for 1 h at 37 °C under stirring. Then, the LipoParticle dispersion was centrifuged at 9000×g for 10 min at 21 °C. Note that the initial L-20K4H-B fluorescent polymer probe amounts were identical in both strategies.

Observation of the Labeled LipoParticles by Bright Field and Fluorescence Microscopy: Observations of the labeled LipoParticles were performed on a wide field microscope Leica DMI6000B using an excitation source Leica Halogen Bulb and an EMCCD camera (Hamamatsu C9100, 512 × 512 pixels, pixel size: 16 µm). A 100× oil immersion objective lens (HCX PL APO Leica, NA = 1.46) was used for both bright field/fluorescence and a BGR filter (450/90; 502/15; 590/20) for fluorescence. On the glass coverslip (170 µm), 10 µL of sample and 2µL of a 5 M NaCl solution were mixed, to decrease the Debye length and favor adhesion of the charged LipoParticles. Images were acquired with LASAF software (Leica, microscope) and Wasabi software (Hamamatsu, camera) and processed with ImageJ freeware.

Cell Culture and Production of HCV Pseudoparticles (HCVpp): Human hepatocarcinoma cells Huh7.5[32,33] were maintained in DMEM containing 4.5 g L⁻¹ D-glucose and 4 × 10⁻³ M L-glutamine (Invitrogen, Cergy-Pontoise, France), supplemented with 100 U mL⁻¹ penicillin, 100 µg mL⁻¹ streptomycin and 10% fetal calf serum (FCS, Lonza). HCV pseudoparticles (HCVpp) were obtained by the transient transfection of 293T cells by the calcium phosphate method. HCVpp of genotype 1a (H77; AF011752) were produced as previously described,[34,35] from 293T cells cotransfected with a murine leukemia virus (MLV) Gag-Pol packaging construct, a MLV-based transfer vector encoding GFP as a reporter protein, and the E1–E2 expression constructs. Supernatants containing pseudoparticles were collected 48 h post-transfection and filtered on 0.45 µm. Pseudoparticles were concentrated 100-fold by ultracentrifugation through a 20% sucrose cushion at 75 000×g for 2 h at 4 °C. Pellets were then resuspended in the Huh7.5 culture medium without FCS.

Labeling of HCVpp with the Fluorescent Polymer Probes: Concentrated HCVpp (200 µL) were incubated with 1 × 10⁻⁶ M polymer probe (final) at 4 °C for 30 min.[36] HCVpp were then placed onto a 20% sucrose cushion, topped with 1 mL phosphate-buffered saline (PBS) and ultracentrifuged at 135 000×g for 1 h 30 min at 4 °C in a TLA-100.4 Beckman rotor. Pellets of labeled virions were resuspended in PBS and stored at 4 °C under dark. Before use for cell infection assays, these pellets were further purified as described in Blaising et al.[4]

Observation of the Labeled HCVpp by TEM, Bright Field and Fluorescence Microscopy: Purified labeled HCVpp were observed by TEM after negative staining with uranyl acetate or phosphotungstic acid (JEOL JEM 1400 microscope at 80 kV, CIQLE facility).

Optical observations were performed on a wide field microscope Leica DM IRBE using an excitation source X-Cite Series 120PC Q and a CCD camera (Hamamatsu C4880, 1280 × 1024 pixels, pixel size: 6 µm). A 63× oil immersion objective lens (HCX PL APO Leica, NA = 1.32) was used for both bright field/fluorescence and a TX2 filter (Excitation 560/40 nm, dichroïc 595 nm, Emission 645/75 nm) for fluorescence. Samples (10 µL) were placed onto a glass coverslip (170 µm). Images were acquired with HIPIC32 software and processed with ImageJ freeware. For some experiments, labeled HCVpp were immuno-stained for Gag retroviral core protein, directly on the glass coverslip.

Observation of Labeled HCVpp after Incubation with Hepatocarcinoma Huh7.5 Cells: Huh7.5 cells were seeded in 12-well plates at 8 × 10⁴ cells *per* well and incubated overnight at 37 °C. Purified labeled HCVpp were then added and plates incubated for 1 h at 4 °C to synchronize viral entry, followed by shift to 37 °C for 10 or 30 min. After supernatant removal and washing in PBS, cells were fixed with methanol (20 min at −20 °C). Observations were performed with a Leica DMI4000 microscope, consisting of a confocal "spinning disk" head (Yokogawa CSU22), an EMCCD camera (Photometrics Quantem 512) and controlled by the Metamorph Software (Molecular Devices). A 63× water immersion objective lens (NA = 1.2) was used. For A-based-polymer probes, the 635 nm laser light was used for excitation and a Cy5 filter set for emission (725/150 nm). Images were processed with ImageJ freeware and Adobe Photoshop. For some experiments, infected fixed cells were immuno-stained on coverslips for Gag retroviral core[4] and clathrin. Imaging was performed using a Leica Confocal Spectral TCS SP5X microscope at 488/30 nm (Dylight 488-labeled antibody), 594/30 nm (Dylight 594-labeled antibody) and 635/40 nm (L-20K3H-A-labeled HCVpp).

HCVpp Infectivity Assay: Huh7.5 cells were incubated with HCVpp, labeled or not, in complete medium for 72 h at 37 °C. The infectious titers, expressed as transducing units (TU) per milliliter, were deduced from the transduction efficiencies, determined as the percentage of cells expressing GFP, measured by FACS analysis.[35]

Supporting Information

Supporting Information is available from the Wiley Online Library or from the author.

Acknowledgements

[1] a) P. Bonnafous, M. Perrault, O. Le Bihan, B. Bartosch, D. Lavillette, F. Penin, O. Lambert, E.-I. Pécheur, *J. Gen. Virol.* **2010**, *91*, 1919; b) C. Faivre-Moskalenko, J. Bernaud, A. Thomas, K. Tartour, Y. Beck, M. Iazykov, J. Danial, M. Lourdin, D. Muriaux, M. Castelnovo, *PLoS One* **2014**, *9*, e83874.

[2] K. E. Coller, K. L. Berger, N. S. Heaton, J. D. Cooper, R. Yoon, G. Randall, *PLoS Pathog.* **2009**, *5*, e1000702.

[3] J. Blaising, P. L. Lévy, S. J. Polyak, M. Stanifer, S. Boulant, E.-I. Pécheur, *Antiviral Res.* **2013**, *100*, 215.

[4] J. Blaising, P. L. Lévy, C. Gondeau, C. Phelip, M. Varbanov, E. Teissier, F. Ruggiero, S. J. Polyak, N. H. Oberlies, T. Ivanovic, S. Boulant, E.-I. Pécheur, *Cell Microbiol.* **2013**, *15*, 1866.

[5] M. Bathfield, F. D'Agosto, R. Spitz, M.-T. Charreyre, T. Delair, *J. Am. Chem. Soc.* **2006**, *128*, 2546.

[6] M. Bathfield, F. D'Agosto, R. Spitz, M.-T. Charreyre, C. Pichot, T. Delair, *Macromol. Rapid Commun.* **2007**, *28*, 1540.

[7] P. Relogio, M. Bathfield, Z. Haftek-Terreau, M. Beija, A. Favier, M.-J. Giraud-Panis, F. D'Agosto, B. Mandrand, J. P. S. Farinha, M.-T. Charreyre, J. M. G. Martinho, *Polym. Chem.* **2013**, *4*, 2968.

[8] M. Bathfield, D. Daviot, F. D'Agosto, R. Spitz, C. Ladavière, M. T. Charreyre, T. Delair, *Macromolecules* **2008**, *41*, 8346.

[9] S. Adjili, A. Favier, J. Massin, Y. Bretonnière, W. Lacour, Y.-C. Lin, E. Chatre, C. Place, C. Favard, D. Muriaux, C. Andraud, M.-T. Charreyre, *RSC Adv.* **2014**, *4*, 15569.

[10] B. Rajwa, T. Bernas, H. Acker, J. Dobrucki, J. P. Robinson, *Microsc. Res. Techniq.* **2007**, *70*, 869.

[11] J. Massin, W. Dayoub, C. Mulatier, C. Aronica, Y. Bretonnière, C. Andraud, *Chem. Mater.* **2011**, *23*, 862.

[12] K. Baathulaa, Y. Xu, X. Qian, *J. Photochem. Photobiol. A* **2010**, *216*, 24.

[13] J. Baumann, M. D. Fayer, *J. Chem. Phys.* **1986**, *85*, 4087.

[14] A.-L. Troutier, C. Ladavière, *Adv. Colloid Interface Sci.* **2007**, *133*, 1.

[15] S. Adjili, A. Favier, G. Fargier, A. Thomas, J. Massin, K. Monier, C. Favard, C. Vanbelle, S. Bruneau, N. Peyriéras, C. Andraud, D. Muriaux, M.-T. Charreyre, *Biomaterials* **2015**, *46*, 70.

[16] K. Nakayama, M. Tamura, *Hepatology* **2010**, *51*, 1083.

[17] A. Quaglia, A. Mustafa, R. R. Mitry, B. Portmann, *Hepatology* **2009**, *50*, 1312.

[18] M. Udagawa, Y. Horie, C. Hirayama, *Biochem. Med.* **1984**, *31*, 131.

[19] A. Codran, C. Royer, D. Jaeck, M. Bastien-Valle, T. F. Baumert, M. P. Kieny, C. A. Pereira, J. P. Martin, *J. Gen. Virol.* **2006**, *87*, 2583.

[20] S. C. Ogden, H. Tang, *Future Virol.* **2015**, *10*, 415.

[21] K.-I. Joo, Y. Lei, C.-L. Lee, J. Lo, J. Xie, S. F. Hamm-Alvarez, P. Wang, *ACS Nano* **2008**, *2*, 1553.

[22] J. Hao, L.-L. Huang, R. Zhang, H.-Z. Wang, H.-Y. Xie, *Anal. Chem.* **2012**, *84*, 8364.

[23] K. C. Nguyen, W. G. Willmoreb, A. F. Tayabali, *Toxicology* **2013**, *306*, 114.

[24] X. Zhao, L. Cai, E. A. Adogla, H. Guan, Y. Lin, Q. Wang, *Bioconj. Chem.* **2015**, *26*, 1868.

[25] F. Li, M. Yang, L. Wang, I. Williamson, F. Tian, M. Qin, P. K. Shah, B. G. Sharifi, *J. Immunol. Methods* **2012**, *386*, 101.

[26] A. Favier, F. D'Agosto, M.-T. Charreyre, C. Pichot, *Polymer* **2004**, *45*, 7821.

[27] C. Chapel, C. Garcia, B. Bartosch, P. Roingeard, N. Zitzmann, F.-L. Cosset, J. Dubuisson, R. A. Dwek, C. Trépo, F. Zoulim, D. Durantel, *J. Gen. Virol.* **2007**, *88*, 1133.

[28] C. Cepraga, T. Gallavardin, S. Marotte, P. H. Lanoë, J. C. Mulatier, F. Lerouge, S. Parola, M. Lindgren, P. L. Baldeck, J. Marvel, O. Maury, C. Monnereau, A. Favier, C. Andraud, Y. Leverrier, M.-T. Charreyre, *Polym. Chem.* **2013**, *4*, 61.

[29] N. Boens, W. Qin, N. Barasic, J. Hofkens, M. Ameloot, J. Pouget, J. P. Lefèvre, B. Valeur, E. Gratton, M. VandeVen, N. D. Silva Jr., Y. Engelborghs, K. Willaert, A. Sillen, A. J. W. G. Visser, A. Van Hoek, J. R. Lakowicz, H. Malak, I. Gryczynski, A. G. Szabo, D. T. Krajcarski, N. Tami, A. Miura, *Anal. Chem.* **2007**, *79*, 2137.

[30] J. Thévenot, A.-L. Troutier, J.-L. Putaux, T. Delair, C. Ladavière, *J. Phys. Chem. B* **2008**, *112*, 13812.

[31] A.-L. Troutier, T. Delair, C. Pichot, C. Ladavière, *Langmuir* **2005**, *21*, 1305.

[32] H. Nakabayashi, K. Taketa, K. Miyano, T. Yamane, J. Sato, *Cancer Res.* **1982**, *42*, 3858.

[33] K. J. Blight, J. A. McKeating, J. Marcotrigiano, C. M. Rice, *J. Virol.* **2003**, *77*, 3181.

[34] D. Lavillette, A. Tarr, C. Voisset, P. Donot, B. Bartosch, A. H. Patel, J. Dubuisson, J. K. Ball, F.-L. Cosset, *J. Virol.* **2005**, *41*, 265.

[35] B. Bartosch, J. Dubuisson, F.-L. Cosset, *J. Exp. Med.* **2003**, *197*, 633.

[36] D. Lavillette, B. Bartosch, D. Nourrisson, G. Verney, F.-L. Cosset, F. Penin, E.-I. Pécheur, *J. Biol. Chem.* **2006**, *281*, 3909.